

Gold(III) dithiocarbamate derivatives of *N*-methylglycine: An experimental and theoretical investigation

Luca Ronconi ^a, Chiara Maccato ^a, Davide Barreca ^b, Roberta Saini ^a,
Mirella Zancato ^c, Dolores Fregona ^{a,*}

^a Dipartimento di Scienze Chimiche, Università di Padova, Via Marzolo 1, 35131 Padova, Italy

^b ISTM-CNR and INSTM, Dipartimento di Scienze Chimiche, Università di Padova, Via Marzolo 1, 35131 Padova, Italy

^c Dipartimento di Scienze Farmaceutiche, Università di Padova, Via Marzolo 5, 35131, Padova, Italy

Received 8 October 2004; accepted 10 December 2004

Abstract

The synthesis and characterization of the gold(III) complexes [(HSDT)AuX₂] and [(HSDT)₂Au]X (X = Cl, Br; HSDT = sarcosinedithiocarbamate (*N*-methylglycinedithiocarbamate)) are reported. In the discussed compounds coordination takes place through the sulfur atoms in a square-planar geometry around the gold(III) metal center. The characterization of the complexes has been carried out by means of elemental analysis, conductance measurements, FT-IR, ¹H and ¹³C NMR spectroscopy, and thermogravimetric analysis. In addition, the molecular structure of the 1:1 metal-to-ligand complexes has been further investigated by means of density functional calculations, confirming the conclusions reached upon application of the other chemical characterization techniques. The complex [(HSDT)₃Au] has been also synthesized and characterized by mass spectrometry, FT-IR, NMR and X-ray photoelectron spectroscopy, even if a definitive determination of its structure has not been undoubtedly accomplished.

© 2005 Elsevier Ltd. All rights reserved.

Keywords: Gold; S ligands; Chelates; Density functional calculations; X-ray photoelectron spectroscopy; Mass spectrometry

1. Introduction

In the widespread scenario of gold organometallic chemistry [1–3], different aspects are receiving increasing attention, such as the study of gold compounds in unusual oxidation states and stereochemistry [4–7], the bioinorganic chemistry of certain gold complexes for the treatment of rheumatoid arthritis (chrysotherapy) and their antitumor and antimicrobial properties [8]. Other research work has been devoted to the synthesis and properties of gold clusters and other complexes with gold–metal bonds [9,10].

In recent years, much interest has been focused on the synthesis of gold(I) derivatives containing sulfur and/or phosphorous donor ligands [11–13]. Among the former, dithiocarbamate complexes have been extensively studied in view of their applications as vulcanization accelerators, flotation agents and pesticides [14,15]; their antimicrobial activity has been reported [16,17] and they have been used to fight against metal poisoning [18].

In the literature, a large number of gold(I) [19,20], gold(III) [20–22] and gold(II) [4,23] dithiocarbamate syntheses are present. In particular, binuclear gold(I) dithiocarbamate derivatives have drawn considerable recent attention due to their significant medical applications or useful optical properties [19c].

The dithiocarbamate moiety has received much attention in recent years due to its ability to act as a bidentate ligand. Dithiocarbamates may easily undergo many

* Corresponding author. Tel.: +39 0 49 8275159; fax: +39 0 2700500560.

E-mail address: dolores.fregona@unipd.it (D. Fregona).

different reactions, thus being useful when studying substitution reactions in cation-bound ligands or between the ligands themselves. The introduction of the dithiocarbamate group in α -amino acids gives rise to molecules with up to three potential bonding residuals: amino ($-\text{NH}_2$, $-\text{NHR}$, $-\text{NHRR}'$), dithiocarbamate ($-\text{CSS}^-$) and carboxylate ($-\text{COO}^-$). Many proteins have cysteine and methionine residuals, which are both characterized by the presence of a sulfur atom in their structure. Consequently, dithiocarbamate derivatives of α -amino acids may be considered as valid models to study the coordination of proteins to metallic cations. Unfortunately, only few literature contributions on the synthesis of such complexes are available up to date [21,24–27].

In this work, compounds formed through reaction of dithiocarbamate derived from *N*-methylglycine (sarcosine) in 1:1, 1:2 and 1:3 metal-to-ligand ratios have been synthesized and characterized by different analytical techniques, in order to gain as much information as possible on their chemico-physical properties. Remarkably, particular attention has been paid to the characterization of 1:3 metal-to-ligand complex, for which a definitive determination of the chemical structure has not been accomplished yet. In the present paper the most relevant experimental and theoretical results are presented and discussed.

2. Experimental

2.1. Apparatus

N-Methylglycine (Aldrich), KAuCl_4 and KAuBr_4 (Alfa Aesar) were used as received. All other reagents and solvents were used as purchased without any further purification.

Conductivity measurements were carried out with an Amel 134-type conductivity bridge for freshly prepared $1.0 \times 10^{-3} \text{ mol L}^{-1}$ solutions in DMSO at $(25.0 \pm 0.1)^\circ\text{C}$.

FT-IR spectra were recorded in nujol between two polyethylene tablets on a Nicolet Vacuum Far FT-IR 20F spectrophotometer for the range $50\text{--}600 \text{ cm}^{-1}$, and in solid KBr on a Nicolet FT-IR 55XC spectrophotometer for the range $400\text{--}4000 \text{ cm}^{-1}$.

^1H NMR spectra were recorded in DMSO-d_6 on a Bruker Avance DRX400 spectrophotometer, equipped with a Silicon Graphics O2 workstation operating in Fourier transform, using tetramethylsilane (TMS) as internal standard. ^{13}C NMR spectra were recorded on the same instrument using TMS as internal standard; proton noise decoupling was normally used to obtain an increase of the observed resonance peaks intensity.

Elemental analyses were performed with a Perkin-Elmer 2400 CHN microanalyser; S, Cl and Br were determined with Schöniger method.

Thermogravimetric and differential scanning calorimetry curves were recorded with a TA Instruments thermobalance equipped with a DSC 2929 calorimeter. Measurements were carried out in the range $25\text{--}1400^\circ\text{C}$ in alumina crucibles under air (flow rate $30 \text{ cm}^3 \text{ min}^{-1}$) at a heating rate of $10^\circ\text{C min}^{-1}$, using alumina as reference.

ESI-MS (electrospray mass spectra) were performed on a Finnegan LCQ ion trap instrument operating in positive ion mode (sheath gas flow N_2 : 50 a.u.; source voltage: 4 kV; capillary voltage: 3 V; capillary temperature: 200°C). $50 \mu\text{L}$ of the sample ($2.9 \times 10^{-3} \text{ mol L}^{-1}$ in TFA/ $\text{H}_2\text{O}/\text{CH}_3\text{CN}$ 1:45:45) were directly injected into the source by a syringe pump with a flow rate of $8.0 \mu\text{L min}^{-1}$.

X-ray photoelectron spectra (XPS) were recorded on a ground sample of $[(\text{HSDT})_3\text{Au}]$ (**6**) by a Perkin-Elmer Φ 5600ci spectrometer at a working pressure of lower than $2.0 \times 10^{-9} \text{ mbar}$ with a monochromatized $\text{AlK}\alpha$ source (1486.6 eV). The spectrometer was calibrated by assuming the binding energy of the $\text{Au}(4f_{7/2})$ line at 84.0 eV with respect to the Fermi level. The standard deviation for the binding energy values was $\pm 0.2 \text{ eV}$. Binding energies were corrected for charging effects by assigning to the C(1s) line of adventitious carbon the value of 284.8 eV [28]. After a Shirley-type background subtraction, the spectra were fitted using a non-linear least-square fitting program, adopting Gaussian-Lorentzian peak shapes. The atomic compositions were evaluated using sensitivity factors as provided by Φ V5.4 A software.

All the computational calculations were performed by running ADF 2002.02 code [29], a program package based on density functional theory (DFT). Calculations were run within the generalized gradient approximation (GGA), with the inclusion of Becke-Perdew exchange-correlation formulas [30,31]. A Triple- ζ Slater-type basis set was used for all the atoms in the system and the relativistic effect was also taken into account by employing the ZORA Hamiltonian which included the scalar relativistic coupling. The inner cores of gold (1s–4d), sulfur (1s–2p), oxygen (1s), carbon (1s) and bromine (1s–3d) were treated by the frozen-core approximation. Furthermore, the harmonic frequencies of the system were calculated by the ADF package employing a numerical differentiation of energy gradients in slightly displaced geometries.

2.2. General procedures and methods

N-Methylglycine (Aldrich), KAuCl_4 and KAuBr_4 (Alfa Aesar) were used as received. All other reagents and solvents were used as purchased without any further purification.

2.2.1. Preparation of the ligand $\text{Ba}(\text{SDT}) \cdot 3\text{H}_2\text{O}$ (**1**)

The dithiocarbamate derivative of the α -amino acid *N*-methylglycine (sarcosine) was prepared as the trihy-

drated barium salt, following a method similar to that described by Musil and Irgolic [35]. *N*-methylglycine (22.95 mmol) was reacted with an aqueous solution (70 ml) of Ba(OH)₂ (22.96 mmol) and the suspension was magnetically stirred until total dissolution was achieved. In order to prevent the precipitation of barium carbonate, the presence of air was avoided, performing the reaction under a nitrogen atmosphere. Acetone was then added until its content was ~40% of the total volume (25 ml), and subsequently CS₂ (22.95 mmol) was dropwise added. Once CS₂ was dissolved, the solution was kept under stirring at 0 °C under a nitrogen flow for 24 h; formation of the barium salt occurred according to the reaction shown in Fig. 1.

Addition of acetone yielded a white precipitate that was filtered off and washed with acetone. The white solid was finally dried in a desiccator with P₄O₁₀, the final yield being 85%. According to the elemental and thermogravimetric analyses, the compound contains three molecules of water of crystallization.

2.2.2. Synthesis of the complexes [(HSDT)AuX₂] (X = Br (2), Cl (4))

An aqueous solution (6 ml) of Ba(SDT) · 3H₂O (0.98 mmol) was treated with a stoichiometric amount of Na₂CO₃ (0.99 mmol), resulting in the formation of a white precipitate (BaCO₃) that was filtered off, and the solution thus obtained was dropwise added to an aqueous solution (2 ml) of KAUX₄ (X = Cl, Br; 0.98 mmol) at 0 °C. The solution was subsequently treated with a stoichiometric amount of a 0.2 mol L⁻¹ solution of HX (X = Cl, Br; 4.92 ml ≅ 0.98 mmol), yielding a reddish-brown precipitate that was filtered off and washed with water and diethyl ether (Fig. 2).

The reddish-brown solid was finally dried in a desiccator with P₄O₁₀, the final yield being 80–90%.

2.2.3. Synthesis of the complexes [(HSDT)₂Au]X (X = Br (3), Cl (5))

1:2 metal-to-ligand gold(III) HSDT derivatives were prepared with a method similar to that of the corresponding 1:1 derivatives. These complexes were obtained by reaction of KAUX₄ (X = Cl, Br) with Ba(SDT) · 3H₂O in a 1:2 molar ratio (KAUX₄/Ba(SD-

T) · 3H₂O = 0.52/1.15 mmol), yielding a reddish-brown powder (final yield: 80–85%).

2.2.4. Synthesis of the complex [(HSDT)₃Au] (6)

An aqueous solution (6 ml) of Ba(SDT) · 3H₂O (1.49 mmol) was treated with a stoichiometric amount of Na₂CO₃ (1.50 mmol), resulting in the formation of a white precipitate (BaCO₃) that was filtered off. The solution thus obtained was cooled and dropwise treated with an aqueous solution (2 ml) of KAUCl₄ or KAUBr₄ (0.49 mmol) at 0 °C (and not dropwise added to the gold(III) salt solution, in order to avoid the formation of the 1:2 metal-to-ligand corresponding derivatives). The solution was subsequently treated with a stoichiometric amount of 0.2 mol L⁻¹ solution of HCl or HBr, respectively (7.42 ml ≅ 1.49 mmol), yielding a dark brown precipitate that was filtered off and washed with water and diethyl ether. The dark brown solid was finally dried in a desiccator with P₄O₁₀, the final yield being 81%.

3. Results and discussion

N-Methylglycinedithiocarbamate has been synthesized as the barium salt as described elsewhere [24,32]. The gold(III) complexes here reported (Fig. 3) have been prepared by adding the dithiocarbamate ligand to an aqueous solution of KAUX₄ (X = Cl, Br) in the appropriate molar ratio.

The analytical data and the conductivity measurements for the ligand and the complexes are reported in Table 1. The compounds are stable at room temperature, insensitive to atmospheric oxygen and moisture and soluble in dimethylsulfoxide (DMSO) only. Conductance measurements are indicative of 1:1 electrolytes for compounds 3 and 5, while compounds 2, 4 and 6 are non-conducting in the same solvent [33–35].

3.1. FT-IR spectroscopy

The most significant bands recorded in the FT-IR spectra of the ligand and the complexes have been reported in Table 2.

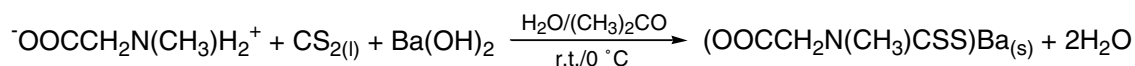


Fig. 1. Synthesis of Ba(SDT) · 3H₂O (1).

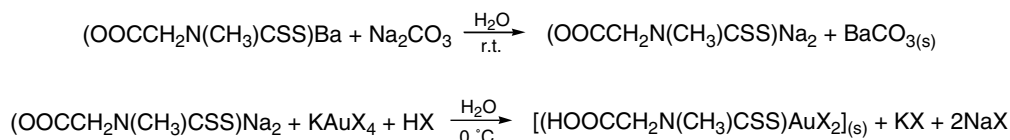


Fig. 2. Synthesis of the complexes 2 and 4.

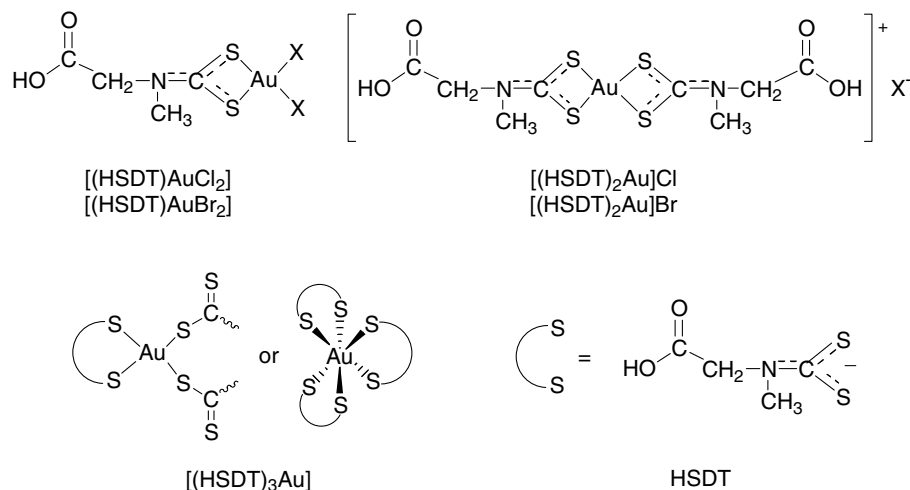


Fig. 3. Chemical drawings of the investigated gold(III) complexes.

Table 1
Analytical data and conductivity measurements [1.0×10^{-3} mol L⁻¹ in DMSO, 25.0 °C]

Compound	Found (calculated)					Λ_M (Ω^{-1} cm ² mol ⁻¹)
	%C	%H	%N	%S	%X (Cl, Br)	
1	13.46 (13.55)	2.98 (3.13)	4.12 (3.95)	17.89 (18.09)		
2	9.24 (9.22)	1.07 (1.16)	2.65 (2.67)	12.68 (12.31)	30.97 (30.67)	1.80
3	15.65 (15.87)	1.75 (2.00)	4.34 (4.63)	21.41 (21.19)	13.24 (13.20)	33.67
4	10.96 (11.12)	1.26 (1.40)	3.17 (3.24)	14.64 (14.84)	16.21 (16.41)	2.02
5	17.23 (17.13)	2.34 (2.16)	4.88 (5.00)	22.33 (22.87)	6.38 (6.32)	33.97
6	21.18 (20.90)	2.71 (2.63)	5.92 (6.09)	27.63 (27.90)		2.14

Table 2
Selected IR frequencies (cm⁻¹)

Compound	$\nu(\text{OH})$	$\nu(\text{N-CSS})$	$\nu(\text{C=O})$	$\nu(\text{C-O})$	$\nu(\text{SCS})$		$\nu(\text{SAuS})$		$\nu(\text{XAuX})$	
					Asym.	Sym.	Asym.	Sym.	Asym.	Sym.
1		1484 _{st}	1570 _{st} ^a	1387 _m ^b	1010 _w	622 _w				
2	3451 _{st,br}	1571 _{st}	1721 _{st}	1216 _{st}	1007 _w	608 _m	384 _{st}	353 _w	248 _{st} ^c	227 _m ^c
3	3429 _{st,br}	1561 _{st}	1718 _{st}	1210 _{st}	1004 _w	608 _m	382 _{st}	357 _{st}		
4	3437 _{st,br}	1569 _{st}	1719 _m	1211 _m	1004 _w	608 _m	381 _{st}	357 _w	336 _m ^d	321 _{sh} ^d
									332 _m ^d	316 _m ^d
5	3446 _{st,br}	1560 _{st}	1718 _m	1209 _{st}	1005 _w	607 _m	380 _{st}	351 _m		
6	3429 _{st,br}	1567 _{st}	1716 _m	1211 _{st}	1004 _w	611 _m	384 _{st}	351 _w		

w = weak; m = medium; st = strong; sh = shoulder; br = broad.

^a $\nu_{\text{as}}(\text{COO}^-)$.

^b $\nu_{\text{s}}(\text{COO}^-)$.

^c X = Br.

^d X = Cl.

The dithiocarbamate compounds exhibit a characteristic band in the range (1450–1580) cm⁻¹ assignable to the N–CSS stretching mode [36–38]; this band defines a carbon–nitrogen bond order intermediate between a single bond ($\Delta\tilde{\nu} = (1250\text{--}1350)$ cm⁻¹) and a double bond ($\Delta\tilde{\nu} = (1640\text{--}1690)$ cm⁻¹) [39]. The presence of a band in the above mentioned range indicates that, of the four possible resonance structures (Fig. 4), in our case we are dealing with a considerable

contribution of structure I, characterized by a strong delocalization of electrons in the dithiocarbamate moiety.

On passing from the dithiocarbamate barium salt to the complexes, the $\nu(\text{N-CSS})$ mode is shifted to higher energies, showing an increase of the carbon–nitrogen double bond character [21,24–26,36]. As regards the halo-derivatives, the $\nu(\text{N-CSS})$ band is shifted to higher frequency following the order



due to the increase of electron withdrawing effects on increasing the number of halide atoms in the complexes, thus promoting an higher positive charge on the nitrogen atom. Thus we can conclude that the contribution of the structure **IV** (Fig. 4) is greater in the bishalo-derivatives and decreases on passing to the monohalo-derivatives, in which the halide atom is just a counter-ion [20].

The most informative bands due to the carboxylic group are recorded between 1200 and 1730 cm^{-1} both for the ligand and the complexes. For the free dithiocarbamate ligand (**1**) two bands are recorded, one for the antisymmetric mode ($\nu_a(\text{COO}^-)$) at 1570 cm^{-1} and another at 1387 cm^{-1} due to the symmetric mode ($\nu_s(\text{COO}^-)$), while the spectra of the complexes show two bands at ~ 1720 and ~ 1210 cm^{-1} due to $\nu(\text{C}=\text{O})$ and $\nu(\text{C}-\text{O})$, respectively. Dithiocarbamates of α -amino acids exhibit bidentate behavior, potentially acting both as S, S' - and O, O' -donors; however, the results discussed above undoubtedly demonstrate that the coordination of the ligand does not take place through the carboxylic group, which maintains its acidic form. This is also confirmed by the presence of a strong broad band at around 3400 cm^{-1} , recorded for all the here investigated complexes, assignable to carboxylic O–H stretching vibrations [40].

The bands due to the –CSS moiety are usually coupled to other vibrations and are very sensitive to the environment of this group, allowing us to distinguish between monodentate and bidentate dithiocarbamate coordination. The presence of only one band in the region (940–1060) cm^{-1} is assumed by Bonati and Ugo [41] to indicate a completely symmetrical bonding of the dithiocarbamate ligand, acting in a bidentate mode (Fig. 5(a)). Conversely, a split band indicates an asymmetrically-bound bidentate ligand ($\Delta\bar{\nu} < 20$ cm^{-1} , Fig. 5(b)) or a monodentate bound ligand ($\Delta\bar{\nu} > 20$ cm^{-1} , Fig. 5(c)). In the complexes here reported, the presence of only one band in the investigated region,

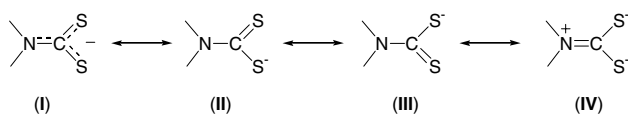


Fig. 4. Resonant forms of the dithiocarbamic –NCSS[−] moiety.

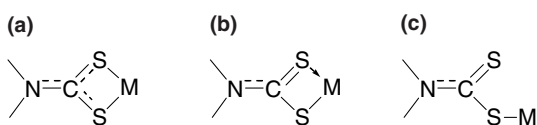


Fig. 5. Different ways of metal–sulfur binding in dithiocarbamate complexes: symmetrical bidentate (a), asymmetrical bidentate (b) and monodentate (c).

commonly attributed to the $\nu_a(\text{SCS})$ vibrational mode, suggests a bidentate symmetrical behavior of the dithiocarbamate moiety, ruling out the coordination schemes 5(b) and (c).

For compound $[(\text{HSDT})_3\text{Au}]$ (**6**) a separate discussion is required. As reported in the literature, gold(III) dithiocarbamate derivatives in a 1:3 metal-to-ligand stoichiometry are generally tetracoordinate in a square-planar geometry with the simultaneous presence of one bidentate and two monodentate dithiocarbamate groups [20]. This case should imply the presence of two well defined N–CSS stretching bands at ~ 1560 and ~ 1450 cm^{-1} due to the bidentate and the monodentate ligands, respectively. In addition, as previously discussed, a split band in the range (940–1060) cm^{-1} , assignable to the $\nu_a(\text{SCS})$, should be recorded, indicating that dithiocarbamate moieties are linked to the central metal ion in different ways [20]. Surprisingly, for compound **6** only one band was observed for both $\nu(\text{N}-\text{CSS})$ and $\nu_a(\text{SCS})$ at 1567 and 1004 cm^{-1} , respectively, indicating the presence of symmetrically bound dithiocarbamate ligands only, acting in a bidentate mode. This experimental evidence led us to hypothesize the possible existence of an hexacoordinate complex, as previously reported for other gold(III) complexes of tris-dithiocarbamate derivatives of α -amino acids [21].

The two bands recorded in the range (350–380) cm^{-1} are ascribed to $\nu_{a,s}(\text{SAuS})$, in agreement with analogous data reported by other authors for similar compounds [37,42].

The bands attributed to the $\nu_{a,s}(\text{XAuX})$ (X = Cl, Br) modes are ascribed to the Au–X stretching frequencies for terminal halides [20,42,43]. The above mentioned metal–halide modes have not been found in the spectra of $[(\text{HSDT})_2\text{Au}]\text{X}$ -type complexes, in agreement with the 1:1 electrolyte character of these compounds. It is worth observing that in the far FT-IR spectra of compound **4** the bands assignable to the $\nu(\text{Au}-\text{Cl})$ vibrations are doubled because of isotopic splitting $\nu(\text{Au}-^{35/37}\text{Cl})$; the existence of only one stable isotope of gold (^{197}Au) helps to make Au–Cl isotopic splitting more easily observable than in the case of chlorides of elements consisting of a mixture of stable isotopes [42].

3.2. ^1H and ^{13}C NMR spectroscopy

The main features of the ^1H and ^{13}C NMR spectra of the ligand and the synthesized complexes have been summarized in Table 3.

All the investigated gold(III) complexes have been proved to be stable in DMSO over 48 h. With regards to the alkyl groups bound to the dithiocarbamate moiety, the ^1H signals are very close for the free dithiocarbamate ligand (**1**) and the corresponding complexes. A general shift towards larger δ values is observed from the free dithiocarbamate precursor to its gold(III)

Table 3
 ^1H and ^{13}C NMR spectral data [DMSO- d_6 , 25.0 °C, ppm]

Compound	^1H NMR		^{13}C NMR			
	CH_3	CH_2	CH_3	CH_2	COOH	CSS
1 ^a	3.36	4.57	43.98	60.46	176.40 ^b	209.73
2	3.38	4.62	35.21	53.11	166.73	193.08
3	3.41	4.63	34.23	52.42	168.15	193.31
4	3.42	4.64	35.87	53.40	166.77	193.42
5	3.42	4.64	34.32	52.60	168.27	193.69
6	3.19	4.49	32.67	46.75	168.17	190.56
	3.48	4.71	34.48	53.64	168.21	195.09

^a Performed in D_2O .

^b Due to the $-\text{COO}^-$ group.

derivatives, probably due to the lower electron density in the complexes, in which the $-\text{NCSS}$ moiety is neutral compared to the free ligand in which such a dithiocarbamic group is anionic [26]. Conversely, for the carbon atoms a significant shielding of the ^{13}C signals, with respect to the free dithiocarbamate ligand, is recorded, in agreement with data reported in the literature for similar compounds [24–26]. The main differences are observable for the ^{13}C signals of the dithiocarbamic carbon atoms. The $\delta(\text{N}^{13}\text{CSS})$ values, falling in the range 190–195 ppm, are strongly dependent on both the type of dithiocarbamate–metal bonding and the oxidation state of the metal center [44]. For gold(III) dithiocarbamate derivatives the $\delta(\text{N}^{13}\text{CSS})$ values, are usually found in the range 193–201 ppm [45].

There is an appreciable empirical correlation between $\delta(\text{N}^{13}\text{CSS})$ values and the carbon–nitrogen stretching vibrations in the infrared spectra: higher $\nu(\text{N}–\text{CSS})$ values indicate an increased carbon–nitrogen double bond character, which well correlates with lower $\delta(\text{N}^{13}\text{CSS})$ values because of a greater electron density on the $-\text{NCSS}$ moiety. For the free dithiocarbamate ligand (**1**), there is no charge compensation on the sulfur atoms by coordinated atoms, resulting in extremely low $\nu(\text{N}–\text{CSS})$ values, correlated with $-\text{N}^{13}\text{CSS}$ signals located in the upper limit of δ values. All these considerations are fully consistent with data reported in Table 3 for $-\text{N}^{13}\text{CSS}$ carbon signals.

As concerns compound **6**, it is worth noting that all the $^1\text{H}/^{13}\text{C}$ resonance peaks are doubled; if the hypothesis of an hexacoordinate complex in solid state was correct, these experimental data would suggest that, in solution, a rapid conversion from hexacoordinate to square-planar geometries could exist (Fig. 6) [21].

The downfield $^1\text{H}/^{13}\text{C}$ signals would be then attributed to the bidentate dithiocarbamate ligand, whereas the upfield ones would be ascribed to the monodentate asymmetrically bound HSdT molecules, as coordination through a single sulfur atom would increase the electron density on the $-\text{NCSS}$ moiety [44].

Finally, the signals due to the carboxylate/carboxylic carbon atoms are generally shifted by ~ 9 ppm to lower

values with respect to the free ligand (**1**), confirming the complete protonation of the carboxylic group, thus leading to an higher electron density on the carboxylic carbon atom [21].

3.3. Thermal studies

The thermal behavior of the free ligand and the synthesized complexes has been studied by thermogravimetry (TG) and differential scanning calorimetry (DSC) techniques in air flow, in order to establish the different decomposition processes and to confirm the proposed stoichiometries. Experimental data agree to a good extent with the ones obtained by the other spectroscopic techniques, and the results of such analysis, summarized in Table 4, indicate a good correlation between calculated and found weight loss values for all the investigated compounds.

As concerns the free dithiocarbamate ligand (**1**), pyrolysis processes take place in two well-defined steps. The first weight loss at around 100 °C coincides with the endothermic DSC peak and corresponds to the loss of three crystallization water molecules. A second weight loss is recorded at higher temperatures (>200 °C), the pyrolysis process leading to the total conversion to the corresponding metallic sulfate (BaSO_4). Several changes in the slope of the TG curve are observed during this second decomposition step, and can be related to the evolution of the hydrocarbon chain as well as to decarboxylation processes [46].

For all the gold(III) dithiocarbamate derivatives **2–6**, the thermal degradation occurs in two successive well-defined steps; in Fig. 7 the thermogram of complex **6** is reported as an example. The first TG step corresponds to pyrolysis, decarboxylation and reductive elimination $\text{Au(III)} \rightarrow \text{Au(I)}$, thus leading to $[\text{Au}(\text{SCN})]$ as a residual, a well known intermediate in the thermal decomposition of metal dithiocarbamates [46,47]. A very intense effect is recorded at higher temperature, that corresponds to removal of the remaining ligand atoms, complete degradation leading to metallic gold [21,25,26]. The formation of metallic gold as the final residual is confirmed by the presence of an endothermic DSC peak at 1066 °C due to the metallic gold melting.

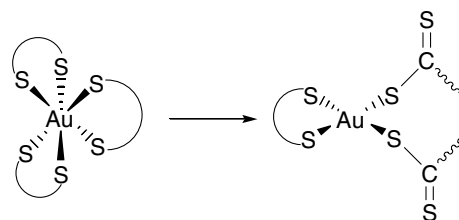


Fig. 6. Hypothesized structural conversion of compound **6** in solution.

Table 4
Thermogravimetric (TG) and differential scanning calorimetry (DSC) data

Compound	Step	Weight loss [%]		DSC
		Found	Calculated	Peak temperature [°C] (process ^a)
1	I	15.81	15.24	102.4 (endo)
	II	34.53	34.18	273.4/326.7/345.7/416.2/762.8 (exo)
2	I	51.42	51.05	192.3 (endo)/263.4 (exo)
	II	61.84	62.19	736.3 (exo)
3	I	57.37	57.87	181.5 (endo)/258.9 (exo)
	II	67.90	67.46	731.1 (exo)
4	I	41.00	40.97	181.9 (endo)/258.1 (exo)
	II	53.98	54.41	737.1 (exo)
5	I	54.28	54.53	183.9 (endo)/248.6 (exo)
	II	64.34	64.88	736.2 (exo)
6	I	63.84	63.02	183.9 (endo)/265.8 (exo)
	II	70.89	71.44	735.7 (exo)

^a Endo/exo = endothermic/exothermic process.

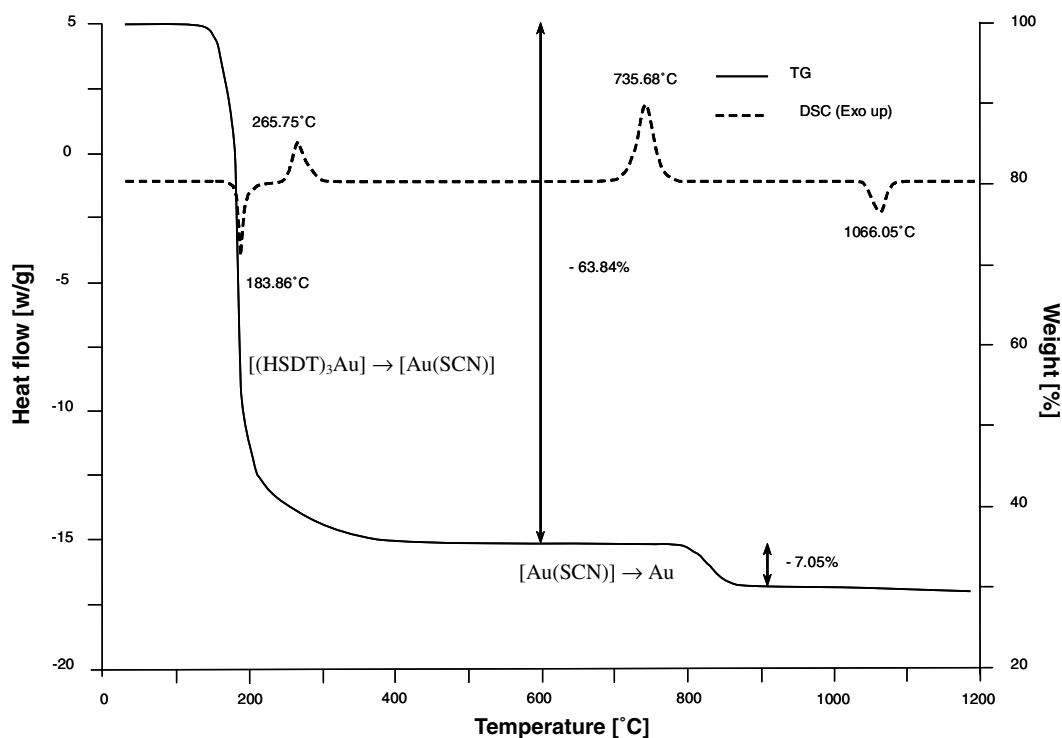


Fig. 7. Thermogram of compound 6.

3.4. Density functional calculations

Aiming to get useful information about the geometrical structures of the compounds here discussed and their harmonic frequencies, we have chosen as a structural starting point of our theoretical investigation the X-ray study of a palladium(II) analogue compound, [(ESDT)Pd(PrNH₂)Cl] (ESDT = ethylsarcosinedithiocarbamate), which presents similar ligands and coordination structure around the metallic center [48].

A ball and stick representation of the optimized complex **2** are reported in Fig. 8(a) and (b). The molecular

scheme of Fig. 8(b) allows us to observe that almost all the molecule lies on the plane pertaining to the square-planar coordination around the metallic center, with the exception of the –COOH moiety. The optimized geometrical parameters and the corresponding literature experimental values of analogue gold(III) complexes [33] are collected in Table 5. Inspection of this table clearly indicates the good agreement between theoretical and available experimental data.

A further point to take into account is the comparison between the calculated harmonic frequencies pertaining to the optimized system and the IR data collected for

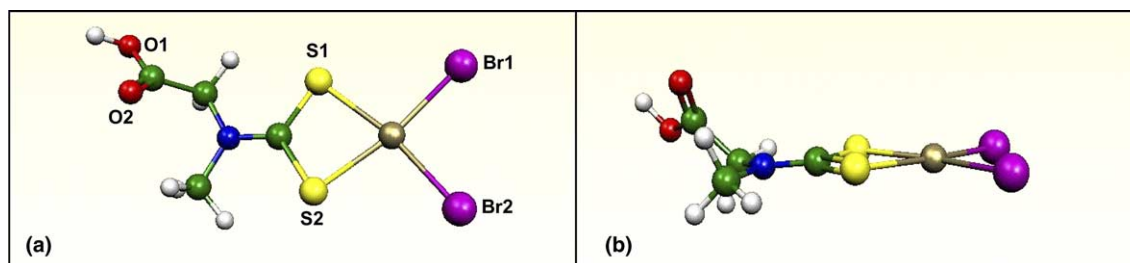


Fig. 8. Ball and stick representation of compound **2** optimized structure: top view (a) and side view (b).

Table 5
Calculated geometrical parameters for compound **2** and literature experimental values

Geometrical parameters	Calculated values	Experimental values [33]
Au–Br1/Br2 (Å)	2.490	2.440
Au–S1 (Å)	2.397	2.373
Au–S2 (Å)	2.392	2.343
C–S1 (Å)	1.737	1.732
C–S2 (Å)	1.732	1.714
N–CSS (Å)	1.341	1.322
N–CH ₃ (Å)	1.469	
N–CH ₂ (Å)	1.457	
CH ₂ –COOH (Å)	1.527	
Br–Au–Br (°)	94.4	
S–Au–S (°)	73.9	74.78
C–S1–Au (°)	86.9	86.1
C–S2–Au (°)	87.1	86.7
N–C–S1 (°)	124.5	124.0
N–C–S2 (°)	123.5	123.6

Table 6
Calculated harmonic frequencies and obtained experimental values for compound **2**

Vibrational features	Calculated frequencies (cm ⁻¹)	Experimental frequencies (cm ⁻¹)
$\nu_s(\text{BrAuBr})$	222	227
$\nu_a(\text{BrAuBr})$	247	248
$\nu_s(\text{SAuS})$	314	353
$\nu_a(\text{SAuS})$	326	384
$\nu_s(\text{SCS})$	787	608
$\nu_a(\text{SCS})$	1095	1007
$\nu(\text{C–O})$	1213	1216
$\nu(\text{N–CSS})$	1426	1571
$\nu(\text{C=O})$	1746	1721

[(HSDT)AuBr₂]; in Table 6 are reported both numerical and experimental vibrational outcomes. The analysis of these data allows us to observe that almost all the calculated frequencies result in good agreement with the experimental ones. We note only one strong discrepancy regarding the values pertaining to –NCSS vibrational modes. This molecular region is probably significantly influenced by the crystal packing in the solid, which was not considered in the theoretical simulation, where we take into account only the full molecular geometry optimization. Consequently, the stretching modes result to be influenced in a different way by the two environments.

Finally, we could get useful information from the values of the Hirshfeld charges collected in Table 7.

The analysis of these data indicates that the gold centre maintains a partial positive charge, while the dithiocarbamic C, N and S atoms result almost neutral; this fact suggests that the π -conjugate electron system on the dithiocarbamate moiety drains charge away from the metallic center.

3.5. Mass spectrometry

The ESI-MS spectrum of complex **6** has been performed in order to clarify its chemical composition. Interpretation of the fragmentation scheme has been a very difficult task. The signal corresponding to the molecular ion was not recorded; the largest m/z value recorded was 525, corresponding to a 1:2 metal-to-ligand fragment. In Fig. 9, a selection of the recorded fragments is reported. One branch of such a scheme represents a series of fragment, all of them including a gold atom, corresponding to successive loss of parts of the ligands, similarly to data reported in the literature [49,50], the last ion recorded having $m/z = 289$, that can tentatively correspond to $[\text{AuS}_2\text{CNH}_2]^+$. The other branch corresponds to withdrawal of a ligand that loses a sulfur atom and, finally, produces a species with $m/z = 87$ that should correspond to $[\text{SCN–C(O)H}]^+$.

3.6. X-ray photoelectron spectroscopy

XPS measurements were carried out on complex **6** in order to obtain a better insight into its chemical composition. The obtained data for the sample agree

Table 7
Hirshfeld charges for selected atoms in compound **2**

Atoms	Hirshfeld charges Q
Br1	–0.25
Br2	–0.25
S1	–0.02
S2	–0.01
N	–0.01
O1	–0.22
O2	–0.15
C(SS)	0.03
Au	0.27

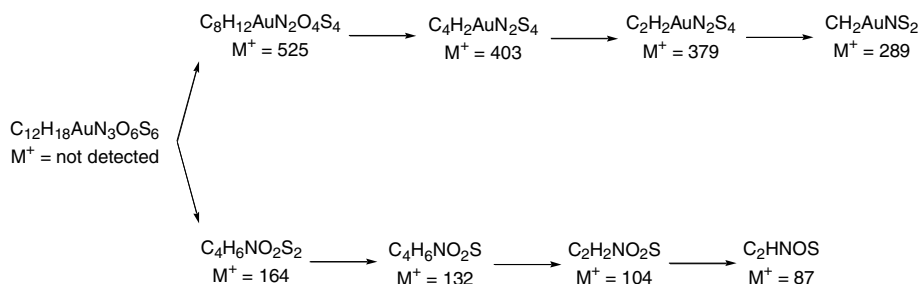


Fig. 9. Selection of the ESI-MS fragments for compound 6.

to a good extent with those obtained by conventional chemical analysis methods, the atomic ratio being Au:O = 0.12/0.14, Au:N = 0.30/0.30, Au:S = 0.21/0.24 and Au:C = 0.05/0.04 (experimental/calculated). Data for the atomic binding energies (BEs) of **6** have been collected in Table 8 together with the full-width at half-maximum (FWHM); these values agree to a good

Table 8
Main XPS data recorded for compound 6

Nucleus	BE (eV)	FWHM
Au 4f _{7/2}	83.8 (Au(I))	2.0
	86.1 (Au(III))	2.0
S 2p _{3/2}	162.1	2.8
N 1s	400.0	2.5
O 1s	531.3	3.1

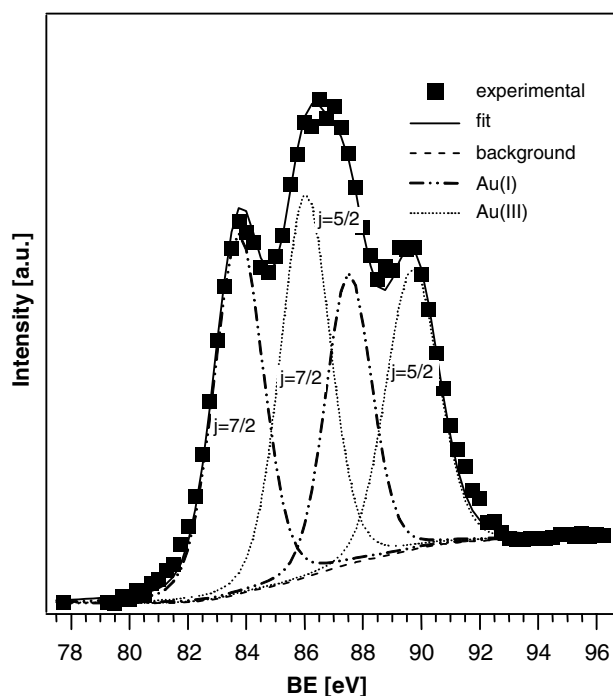


Fig. 10. Deconvolution of the Au(4f) photoelectron peak for compound 6.

extent with those reported in the literature for analogous gold(III) complexes of tris-dithiocarbamate derivatives of α -amino acids [21,51,52].

The Au(4f_{7/2}) peak analysis required greater attention. The recorder photoelectron signal, together with the bands resulting from the least-squares fitting, is reported in Fig. 10. As a matter of fact, such a signal can be decomposed by means of two distinct doublets, whose Au(4f_{7/2}) components are located at BE = 83.8 eV (FWHM = 2.0 eV) and BE = 86.1 eV (FWHM = 2.0 eV). These bands can be ascribed to the presence of gold(I) and gold(III), respectively [53], the former resulting from a partial reduction of gold(III) species in the spectrometer chamber due to the XPS analysis conditions [54–56].

The fact that only one S(2p) signal is recorded could support the hexacoordinate geometry, against a square-planar geometry reported in the literature for some other gold(III) dithiocarbamate derivatives with a 1:3 metal-to-ligand stoichiometry [20]. For square-planar 1:3 complexes, one of the ligands would act as bidentate and the other two as monodentate, coordinating the gold(III) center through one sulfur atom. In such a case, three different signals due to S(2p) orbitals would be expected (that is, one due to sulfur atoms implied in the bidentate coordination, one due to coordinating sulfur atoms belonging to monodentate ligands, and another due to the free sulfur atoms of the monodentate ligand). Indeed, only one single S(2p) signal is recorded in our case. Anyway, at variance with the report by Criado et al. [21], we do not believe that these data alone can support the presence of an hexacoordinate gold(III) geometry in the analyzed complex [(HSDT)₃Au]. This claim would be also disproved by the results of density functional calculations.

4. Conclusions

In this paper we report on the synthesis and characterization of five gold(III) dithiocarbamate derivatives of the type [(HSDT)₂AuX₂], [(HSDT)₂Au]X and [(HSDT)₃Au] (X = Cl, Br; HSDT = *N*-methylglycine-dithiocarbamate).

Although none of the complexes here reported has been obtained in the crystalline state, and thus the structure cannot be undoubtedly proposed, the other results suggest that coordination of the 1:1 and 1:2 metal-to-ligand dithiocarbamate derivatives takes place in a near square-planar geometry through the sulfur donating atoms, the –NCSS moiety coordinating the metal atom in a bidentate symmetrical mode and lying in the same plane, as reported in the literature for analogous gold(III) complexes.

A particular case is that of compound [(HSDT)₃Au] whose structure has not been undoubtedly accomplished. Experimental results seem to support the hypothesis of an hexacoordinate tris-dithiocarbamate gold(III) derivative, against a square-planar geometry generally proposed for gold(III) complexes in a 1:3 metal-to-ligand stoichiometry.

Acknowledgements

The authors gratefully acknowledge partial financial support of this work by *Ministero dell'Università e della Ricerca Scientifica e Tecnologica* (Pharmacological and diagnostic properties of metal complexes).

References

- [1] R.J. Puddephatt, in: G. Wilkinson, F.G.A. Stone, E.W. Abel (Eds.), *Comprehensive Organometallic Chemistry*, vol. 2, Pergamon, Oxford, 1982, p. 765.
- [2] A. Grahmann, H. Schmidbaur, in: E.W. Abel, F.G.A. Stone, G. Wilkinson (Eds.), *Comprehensive Organometallic Chemistry II*, vol. 3, Pergamon, Oxford, 1995, p. 1.
- [3] M.C. Gimeno, A. Laguna, *Gold Bull.* 36 (2003) 83.
- [4] L.V. Antonova, T.E. Busygina, V.K. Polovnyak, A.E. Usachev, *Russ. J. Gen. Chem.* 67 (1997) 529.
- [5] I.C. Hwang, K. Seppelt, *Angew. Chem., Int. Ed.* 40 (2001) 3690.
- [6] D. Belo, H. Alves, E.B. Lopes, M.T. Duarte, V. Gama, R.T. Henriques, M. Almeida, A. Perez-Benitez, C. Rovira, J. Veciana, *Chem. Eur. J.* 7 (2001) 511.
- [7] V.W.W. Yam, C.K. Li, C.L. Chan, K.K. Cheung, *Inorg. Chem.* 40 (2001) 7054.
- [8] E.R.T. Tiekink, *Crit. Rev. Oncol. Hematol.* 42 (2002) 225.
- [9] H.X. Zhang, C.M. Che, *Chem. Eur. J.* 7 (2001) 4887.
- [10] L. Mezailles, N. Avarvari, N. Maigrot, L. Ricard, F. Mathey, P. LeFloch, L. Cataldo, T. Berclaz, M. Geoffroy, *Angew. Chem., Int. Ed.* 38 (1999) 3194.
- [11] H. Schmidbaur, G. Weidenhiller, O. Steigelmann, *Angew. Chem., Int. Ed.* 30 (1991) 433.
- [12] A. Sladek, K. Angermaier, H. Schmidbaur, *Chem. Commun.* (1996) 1959.
- [13] J.P. Fackler Jr., *Inorg. Chem.* 41 (2002) 6959.
- [14] A. Lopez Garcia, E. Blanco Gonzales, A. Sanz-Medel, *Chromatographia* 43 (1996) 607.
- [15] A.L.J. Rao, N. Verma, A. Kumar, J. Kapoor, *Chem. Environ. Res.* 4 (1995) 163.
- [16] E.M. Walker, H.F. Hardin, G.L. Gale, M.E. Reifsteck, D.J. Cannon, M.M. Jones, *Res. Common Chem. Pathol. Pharmacol.* 63 (1989) 101.
- [17] S. Sarac, M. Ertan, A. Balkan, N. Yulua, *Arch. Pharm. Weinheim* 324 (1991) 449.
- [18] F. Caruso, M.L. Chan, M. Rossi, *Inorg. Chem.* 36 (1997) 3609.
- [19] (a) M. Bardaji, A. Laguna, M. Laguna, *J. Chem. Soc., Dalton Trans.* (1995) 1255;
(b) M. Bardaji, A. Laguna, M. Laguna, F. Merchán, *Inorg. Chim. Acta* 215 (1994) 215;
(c) E.J. Fernandez, J.M. Lopez-de-Luzuriaga, M. Monge, E. Olmos, M.C. Gimeno, A. Laguna, P.G. Jones, *Inorg. Chem.* 37 (1998) 5532.
- [20] F. Forghieri, C. Preti, L. Tassi, G. Tosi, *Polyhedron* 7 (1988) 1231.
- [21] J.J. Criado, J.A. Lopez-Aria, B. Macías, L.R. Fernandez-Lago, J.M. Salas, *Inorg. Chim. Acta* 193 (1992) 229.
- [22] R.V. Parish, B.P. Howe, J.P. Wright, J. Mack, R.C. Pritchard, R.G. Buckley, A.M. Elsome, S.P. Fricker, *Inorg. Chem.* 35 (1996) 1659.
- [23] M. Bardaji, M.C. Gimeno, P.G. Jones, A. Laguna, M. Laguna, *Organometallics* 13 (1994) 3415.
- [24] M. Castillo, J.J. Criado, B. Macías, M.V. Vaquero, *Inorg. Chim. Acta* 124 (1986) 127.
- [25] J.J. Criado, A. Carrasco, B. Macías, J.M. Salas, M. Medarde, M. Castillo, *Inorg. Chim. Acta* 160 (1989) 37.
- [26] J.J. Criado, I. Fernandez, B. Macías, J.M. Salas, M. Medarde, *Inorg. Chim. Acta* 174 (1990) 67.
- [27] B. Macías, J.J. Criado, M.V. Villa, M.R. Iglesias, M. Castillo, *Polyhedron* 12 (1993) 501.
- [28] D. Briggs, M.P. Seah, *Practical Surface Analysis*, John Wiley & Sons, Chichester, 1983.
- [29] H.H. Murray, G. Garzon, G. Raptus, A.M. Mazany, L.G. Porter, J.P. Fackler, *Inorg. Chem.* 27 (1988) 836.
- [30] A.D. Becke, *Phys. Rev. A* 38 (1988) 3098.
- [31] J.P. Perdew, *Phys. Rev. B* 33 (1986) 8822.
- [32] A. Musil, K. Irgolic, *Z. Anal. Chem.* 208 (1965) 352.
- [33] J.A. Broomhead, L.A.P. Kone-Maguire, *J. Chem. Soc. A* (1967) 546.
- [34] N.N. Greenwood, B.P. Straughon, A.E. Wilson, *J. Chem. Soc. A* (1968) 2209.
- [35] L.A.P. Kone-Maguire, P.S. Sheridan, F. Basolo, R.G. Pearson, *J. Am. Chem. Soc.* 90 (1968) 5295.
- [36] S. Wajda, K. Drabent, *Bull. Acad. Polon. Sci., Sci. Chim.* 25 (1977) 963.
- [37] N. Nakamoto, J. Fujita, R.A. Condrote, Y. Morimoto, *J. Chem. Phys.* 39 (1963) 42.
- [38] G. Durgaprasad, D.N. Sathyanarayana, C.C. Patel, *Can. J. Chem.* 47 (1969) 631.
- [39] A.W. Herlinger, S.N. Wenholt, T.V. Long, *J. Am. Chem. Soc.* 92 (1970) 6474.
- [40] R.M. Silverstein, F.X. Webster, *Spectrometric Identification of Organic Compounds*, 6th ed., Wiley, New York, 1998.
- [41] F. Bonati, R. Ugo, *J. Organomet. Chem.* 10 (1967) 257.
- [42] P.T. Beurskens, H.J.A. Bloaw, J.A. Cras, J.J. Steggerda, *Inorg. Chem.* 7 (1968) 805.
- [43] G.E. Coates, C. Parkin, *J. Chem. Soc.* (1963) 421.
- [44] H.L.M. van Gaal, J.W. Diesveld, F.W. Pijpers, J.G.M. van der Linden, *Inorg. Chem.* 18 (1979) 3251.
- [45] J. Willemse, J.A. Cras, J.J. Steggerda, C.P. Keyzers, *Struct. Bond.* (Berlin) 28 (1976) 83.
- [46] B. Macías, J.J. Criado, M.V. Vaquero, M.V. Villa, *Thermochim. Acta* 223 (1993) 213.
- [47] A. Fernandez-Alba, I.J. Perez-Alvarez, J.L. Martinez-Vidal, E. Gonzalez-Pradas, *Thermochim. Acta* 211 (1992) 271.
- [48] G. Faraglia, D. Fregona, S. Sitran, L. Giovagnini, C. Marzano, F. Baccichetti, U. Casellato, R. Graziani, *J. Inorg. Biochem.* 83 (2001) 31.
- [49] T. Tetsumi, M. Sumi, M. Tanaka, T. Shono, *Polyhedron* 5 (1986) 706.
- [50] A.M. Bond, R. Colton, D.R. Mann, *Inorg. Chem.* 29 (1990) 4665.

- [51] G. Furlani, G. Polzonetti, C. Preti, G. Tosi, *Inorg. Chim. Acta* 73 (1983) 105.
- [52] G. Polzonetti, C. Preti, G. Tosi, *Polyhedron* 5 (1986) 1969.
- [53] J.F. Mulder, W.F. Stickle, P.W. Sobol, K.D. Bomben, *Handbook of X-ray Photoelectron Spectroscopy*, Perkin–Elmer Corporation, MN, 1992.
- [54] P.M.T. van Attekum, J.M. Trooster, *J. Chem. Soc., Dalton Trans.* (1980) 261.
- [55] R.G. Raptis, L.C. Porter, R.J. Emrich, H.H. Murray, J.P. Fackler Jr., *Inorg. Chem.* 29 (1990) 4408.
- [56] R.G. Raptis, J.P. Fackler Jr., *Inorg. Chem.* 29 (1990) 5003.